Grain-boundary effects on magnetotransport in $La_{0.7}Sr_{0.3}MnO_3$ biepitaxial films

R. Mathieu and P. Svedlindh
Department of Materials Science, Uppsala University, Box 534, SE-751 21 Uppsala, Sweden

R. A. Chakalov* and Z. G. Ivanov
Department of Physics, Chalmers University of Technology, SE-412 96 Göteborg, Sweden
(Received 3 December 1999; revised manuscript received 15 March 2000)

The low field magnetotransport of $La_{0.7}Sr_{0.3}MnO_3$ (LSMO) films grown on $SrTiO_3$ substrates has been investigated. A high quality LSMO film exhibits anisotropic magnetoresistance (AMR) and a peak in the magnetoresistance close to the Curie temperature of LSMO. Biepitaxial films prepared using a seed layer of MgO and a buffer layer of CeO_2 display a resistance dominated by grain boundaries. One film was prepared with seed and buffer layers intact, while a second sample was prepared as a 2D square array of grain boundaries. These films exhibit (i) a low temperature tail in the low field magnetoresistance, (ii) a magnetoconductance with a constant high field slope, and (iii) a comparably large AMR effect. A model based on a two-step tunneling process, including spin-flip tunneling, is discussed and shown to be consistent with the experimental findings of the biepitaxial films.

I. INTRODUCTION

In recent years much attention has focused on the magnetoresistive properties of hole doped manganite perovskites.[1] In case of single crystals[2] and high quality epitaxial films,[3–7] the magnetoresistance effect is large only close to the ferromagnetic transition temperature. Moreover, comparably large applied fields, of order 1 T, are required to obtain a sizeable effect, which makes it difficult to exploit these materials in for instance sensor applications. It has been suggested that transport is of activated form with a hopping motion of carriers forming polarons. Also, a strong transport-magnetism correlation has been observed both above and below the Curie temperature.[3,4]

A large low field magnetoresistance is known to exist in polycrystalline bulk ceramic materials[8,9] as well as in thin films containing interfaces and grain boundaries of some kind.[2,5–7,10,12,13] Experimental realizations of the latter include polycrystalline films,[2,6,10,11] films grown on bicrystal substrates with different grain boundary angles,[5,12,14] step-edge structures,[7] and trilayer junction structures.[10,11] Models proposed to explain this low field effect include spin-polarized tunneling,[9,15–19] spin dependent scattering at grain boundaries–domain walls,[13] and activated carrier transport in grain-boundary regions.[20]

In this paper, we study the magnetic and magnetoresistive properties of a 2D array (2DA) of weakly coupled LSMO islands. Its properties are compared with two reference samples: an epitaxial LSMO film (EF) and a LSMO film with irregular grain boundaries (GBF). Both 2DA and GBF were prepared as biepitaxial films and exhibit a similar and strong effect of grain boundaries on the magnetoresistive behavior. Still, differences in behavior are observed when studying the anisotropy of the magnetoresistance. Below magnetic saturation, the anisotropic magnetoresistance in case of 2DA contains an extrinsic contribution from the geometry of the grain boundaries. It is argued that a model based on a two-step inelastic tunneling process can account for the magnetoresistive behavior of the two biepitaxial films.

II. SAMPLES AND EXPERIMENTS

Three $La_{0.7}Sr_{0.3}MnO_3$ (LSMO) ($a_{LSMO}=3.82$ Å) thin films grown on $SrTiO_3$ (STO) substrates ($a_{STO}=3.905$ Å) have been investigated: A high quality epitaxial film (EF) and two bi-epitaxial films. Structural properties of the films were checked with x-ray θ-2θ and ϕ scans. Details on the fabrication process and characterization are described elsewhere.[21] The epitaxial film is highly *c*-axis oriented and only [100] LSMO ∥[100] STO in-plane orientation is observed. The biepitaxial[23] films were prepared by using a seed layer of MgO ($a_{MgO}=4.21$ Å) having a thickness of 20 nm and a buffer layer of CeO_2 ($a_{CeO}=5.41$ Å). One film sample (GBF) was prepared with seed and buffer layers intact, while a second sample (2DA) was prepared as a 2D square array of grain boundaries. To form this array, the MgO seed layer was etched into a chess board pattern with fields of $8\times8\,\mu m^2$. The chess board fields, where the STO surface is disclosed, initiate a 45° in-plane rotated growth of the CeO_2 buffer layer. The LSMO inherits the template orientation of the buffer layer forming 45° misoriented domains as well as a 500×500 array of 45° grain boundaries (GB). Figure 1 shows a schematic representation of 2DA as well as an AFM image of the chess board fields. ϕ scans reveal a predominant [100] CeO_2∥ [100] MgO growth of the buffer layer, but with a fraction of [110] CeO_2∥ [100] MgO orientations. In addition, some small fraction of grains having a mutual misorientation angle of $\pm24°$ was detected. From this it is clear, since LSMO inherits the orientaion of CeO_2, that GBF also will contain GB of the kind indicated by the ϕ scans.

There is limited data on the structure of GB in LSMO. We have performed detailed TEM studies on a 20° GB grown on a $LaAlO_3$ bicrystal substrate.[22] The two parts of the LSMO film on the bicrystal substrate form a sharp on an atomic

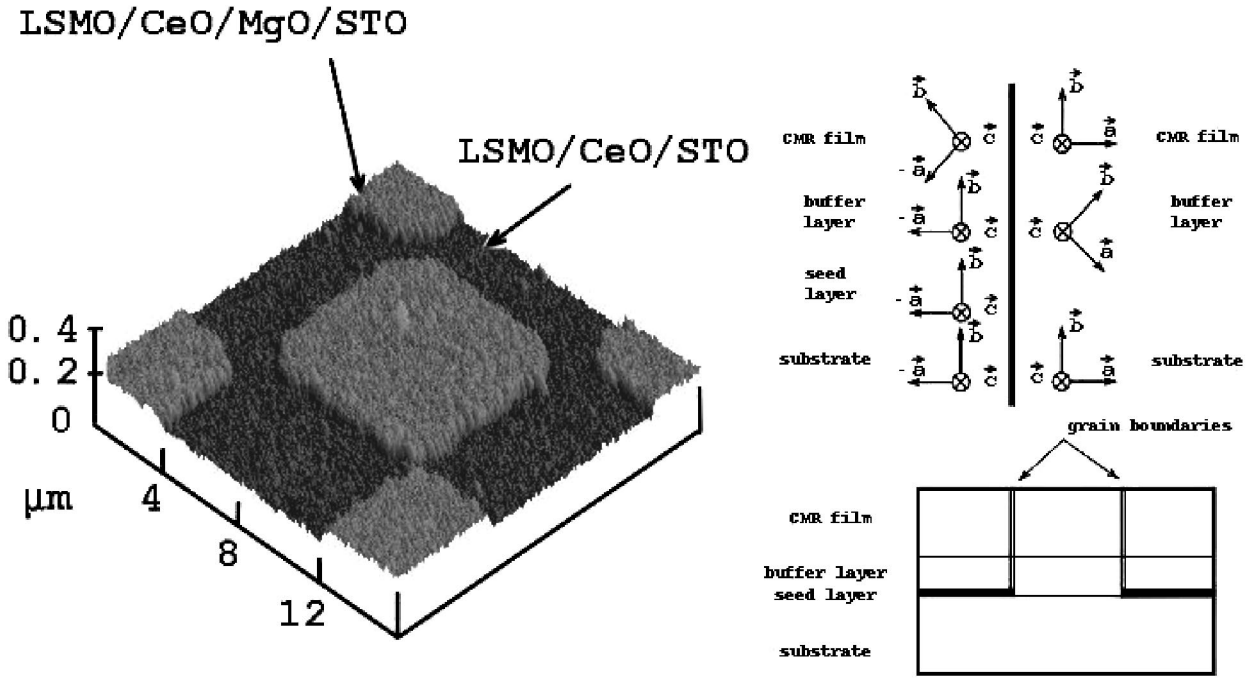

FIG. 1. An AFM image of 2DA and a schematic representation of the orientation of the different layers of this biepitaxial structure.

scale symmetrical GB. However, facets parallel to the low index crystallographic planes of the LSMO are present. The GB consists of closely spaced edge dislocations with a periodicity of 4–5 LSMO unit cells (1.6–2 nm). No impurity phases are detected at the GB. Although we have not investigated the 45° GB in 2DA, from the results on the 20° GB, we expect the 45° GB to have a similar structure but with even closer spaced edge dislocations. The disorder at the GB can be estimated to have a thickness of 3–5 nm in the LSMO layer.

Magnetization $M(H,T)$ measurements were performed in a Quantum Design SQUID magnetometer. The resistivity $\rho(H,T,\theta)$ was measured using a standard four-probe method and a Maglab 2000 system from Oxford Instruments with a rotationary probe. The magnetoresistance of the samples is defined as $[R_0-R_H(\theta)]/R_0$; the angle θ refers to the angle between the current and the in-plane applied magnetic field.

III. RESULTS FROM MAGNETIC AND TRANSPORT MEASUREMENTS

Figure 2 shows the temperature dependence of the magnetization for all samples. Zero-field cooled (ZFC) and field cooled (FC) magnetizations with a magnetic field of 4 kA/m are shown. All films exhibit ferromagnetic order at low temperature with approximately the same Curie temperature $T_c \approx 360$ K, in agreement with results from earlier studies on LSMO films with optimum hole doping.[24] The low field magnetization below T_c is larger for EF than for the other two samples. This is expected, considering the high crystalline quality of this sample, since reversible and irreversible domain wall motions determine the magnitude of the low field magnetization. For 2DA, the magnetization remains large and approximately constant above T_c, indicating some kind of magnetic order remaining in the sample even at these high temperatures, a conclusion which is further supported by the hysteresis curve shown in the inset of Fig. 2. X-ray diffraction reveals no impurity phases, suggesting a real two-step magnetic transition. This peculiarity of the 2DA sample is not fully understood; it could be related to the specific properties of this kind of grain boundary. The previously discussed study of a 20° bicrystal GB revealed a regular set of edge dislocations with a period of 4–5 unit cells and strong stress fields at the grain boundary.[22] These two factors may contribute to the observed high temperature magnetic ordering. The origin of this ordering is however left for further studies where the size of the chess board fields will be varied, thereby changing the relative amount of distorted film material.

The field dependence of the magnetization was studied at different temperatures in the range 5 K to 200 K. Typical hysteresis curves are shown in Fig. 3 for $T=5$ K. For EF, the hysteresis curve is rather square shaped, as in a sample

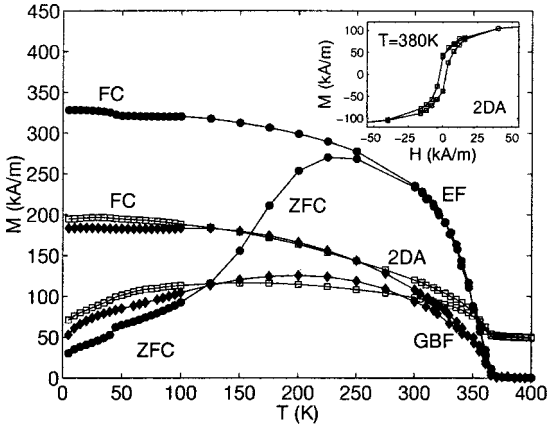

FIG. 2. ZFC and FC magnetization for EF (filled circles), GBF (filled diamonds) and 2DA (open squares); $H=4$ kA/m. The inset shows the hysteresis loop for 2DA at $T=380$ K.

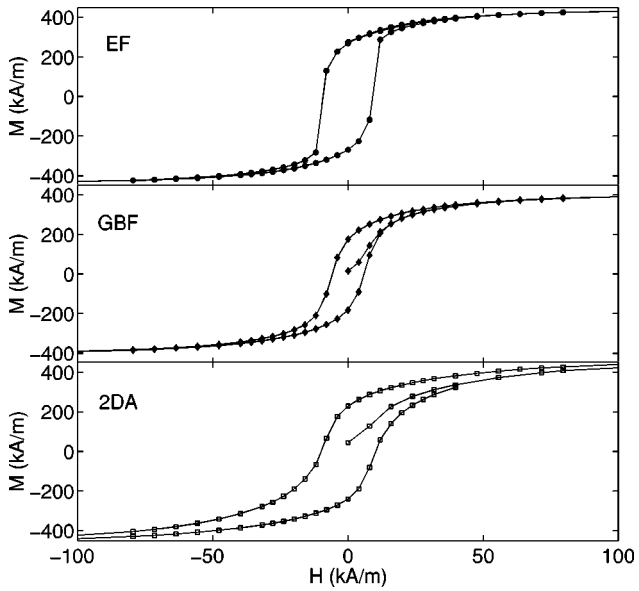

FIG. 3. Hysteresis loops at $T=5$ K for the EF (filled circles), GBF (filled diamonds) and 2DA (open squares) samples.

with no (or few) defects, confirming the excellent epitaxial growth. GBF contains some amount of grain boundaries; as a result, the hysteresis curve is more inclinated. Also one notices that the addition of defects in the form of grain boundaries promote the nucleation of reversed domains, thereby reducing the coercivity. Adding more boundaries as is the case for the chess board film, the hysteresis curve becomes even more inclinated, but the coercivity increases, indicating a pinning controlled mechanism for the coercivity in this sample. These general characteristics remain at higher temperatures. Figure 4 presents the zero magnetic field resistivity of the two biepitaxial films, with the results for EF as an inset for comparison. The behavior of the bi-epitaxial films is very different from that of EF, with no significant features at T_c. Broad maxima in the resistivity are present well below T_c, like in the resistivity curves obtained using a Wheatstone bridge geometry on $La_{0.7}Sr_{0.3}MnO_3$ bicrystal meander-patterned films to measure directly the grain boundary resistivity,[20] indicating a grain boundary dominated resistivity for the two biepitaxial films.

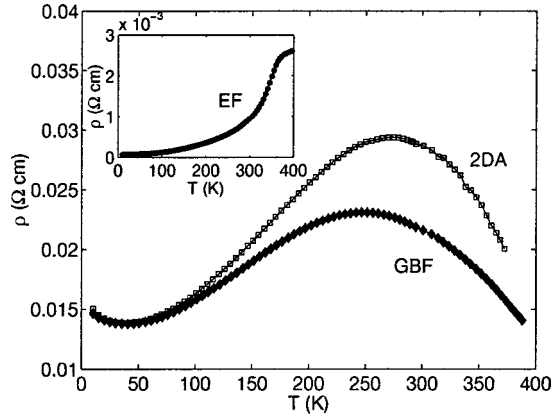

FIG. 4. Temperature dependence of the zero field resistivity for the two biepitaxial films. The inset shows the corresponding result for EF.

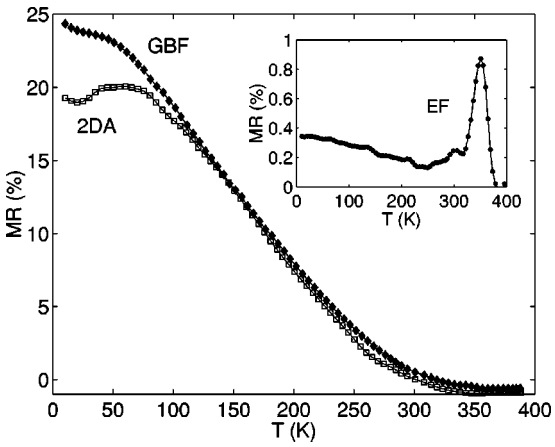

FIG. 5. Temperature dependence of the low field magnetoresistance ($\mu_0 H=0.1$ T) for the two bi-epitaxial films. The inset shows the corresponding result for EF.

Figure 5 shows the temperature dependence of the low field magnetoresistance (for $\mu_0 H=0.1$ T) for the two biepitaxial films, with the corresponding result for EF as an inset in the same figure. EF displays the typical low field magnetoresistance behavior for a high quality epitaxial film,[3–7,25,26] with a peak in the magnetoresistance around T_c, and no significant low temperature MR. To observe a ''colossal'' magnetoresistance in this sample, much larger fields are needed; the MR is 10% at RT applying a field of 5 T. These results are typical for single crystals and high quality epitaxial films of LSMO.[20] Due to the strong transport-magnetism correlations seen in high quality CMR films, the conduction is thought to correspond to activated (magnetic) polaron hopping,[1,3,4,27] even though other mechanisms like reduction of spin fluctuations have been suggested to account for the MR effect.[2,28] In comparison, the biepitaxial films exhibit a low temperature tail with an increasing low field magnetoresistance with decreasing temperature. No significant features appear at T_c. On the one hand, the absence of a magnetoresistance peak around T_c can be attributed to grain boundary stress fields and/or stoichiometry variations,[20] which will change the Curie temperature close to the grain boundary or may even locally create a different type of magnetic order. It is to be expected that the different types of grain boundaries existing in the biepitaxial films are associated with distributions of stress fields (and stoichiometry variations) and hence distributions of grain boundary Curie temperatures, thereby erasing the sharp magnetoresistance peak around the measured T_c. On the other hand, the low temperature raise of the magnetoresistance is attributed to a different transport mechanism such as spin polarized tunneling through a barrier region, something which will be discussed in more detail below.

Figure 6(a) shows the high field behavior of the magnetoresistance for 2DA at different temperatures, from $T=10$ K to $T=300$ K, and Fig. 6(b) the low-field behavior for different orientations of the in plane magnetic field ($H \| I$ and $H \perp I$); similar features were observed for the GBF film. The high field resistance at first sight looks linear with the magnetic field [cf. Fig. 6(a)], but, as will be discussed later, it is the high field conductance that exhibits a linear high field regime. 2DA also shows magnetoresistance hysteresis

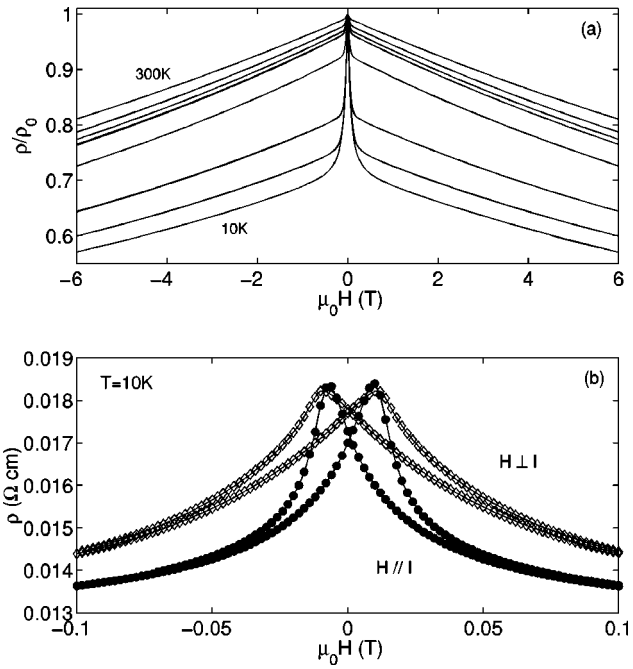

FIG. 6. Field dependence of the resistivity of 2DA for high fields (a) and low fields (b). For high fields, the normalized resistivity is shown for $T=10, 50, 100, 200, 250, 260, 275$, and 300 K; for clarity, only 10 K and 300 K are marked in the figure. In the low field case, hysteresis loops are shown for $T=10$ K with the applied magnetic field parallel and perpendicular to the current.

at low fields [cf. Fig. 6(b)], commonly related to defects and grain boundaries in the films; the peak resistance occurs at a field near to the coercive field. The hysteretic behavior remains at higher temperatures. One also notices that, as has been reported for structures with well oriented grain boundaries,[20] a higher MR effect is obtained for $H \| I$.

If the previously discussed features were expected, considering the presence of grain boundaries, peculiar orientation-dependent effects appear for the biepitaxial films. In Fig. 7, resistivity vs θ, angle between the applied magnetic field and current, is presented for the two biepitaxial films at $T=80$ K and $\mu_0 H=0.05$ T [Figs. 7(a) and 7(b)]. Both samples exhibit anisotropic magnetoresistance (AMR). Sinusoidal $\alpha_2 \sin(2\theta)$ fits are included; the residue subtracting the fit from the experimental result is shown in Figs. 7(c) and 7(d). For 2DA, a new sinusoidal fit of the residue has been added, suggesting an additional $\alpha_4 \sin(4\theta)$ periodic contribution. This term disappears when increasing the magnetic field above the saturation field of the sample (Fig. 8), at which fields the AMR amplitude also saturates; the high field AMR is $\approx 1.5\%$. The residue for GBF is smaller, but still suggests contributions from higher frequency angular terms. Fourier analysis of the angular dependence of the magnetoresistance allows us to resolve (at least) 2θ, 4θ, and 6θ terms; for the GBF film $\alpha_2 >> \alpha_{i>2}$, while for the 2DA film α_4 and α_6 are comparably large (approximately 1/10 of α_2). The AMR in EF is rather much smaller as compared to that displayed in Fig. 7; the low temperature, high field AMR is only about 0.2–0.3 %. Still, a Fourier analysis of the angular dependence of the magnetoresistance for this film shows a behavior similar to that of 2DA; at low fields 2θ, 4θ, and 6θ terms can be resolved while for fields larger than the saturation field only the 2θ term is seen. One the one hand, the high field AMR is an intrinsic property of LSMO associated with spin-orbit coupling.[29,30] On the other hand, the low field AMR contains an extrinsic contribution from the geometry of the grain boundaries as well as a contribution originating from, and having the same symmetry as, the magnetic anisotropy. Below but close to saturation, the induced magnetization will be modulated as determined by the symmetry of the magnetic anisotropy when the film is rotated with respect to the applied field.

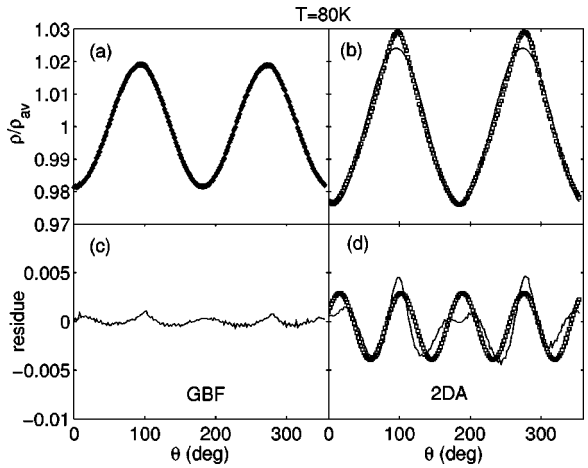

FIG. 7. Angular dependence of the resistivity for the two biepitaxial films; $\mu_0 H=0.05$ T. The normalized resistivity is fitted by a sinuisoidal function [(a) and (b)], and the residue subtracting the fit from the experimental data is shown in (c) and (d). In (d) an additional sinusoidal fit of the residue is included.

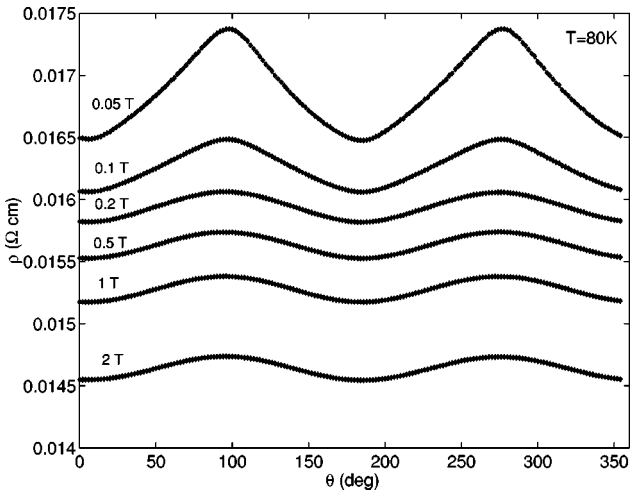

FIG. 8. Field dependence of the AMR for 2DA.

IV. DISCUSSION

It is clear that one additional transport mechanism is present in films containing grain boundaries as compared to high quality epitaxial films. A model attempting to describe the properties of the biepitaxial films must be able to account for; (i) the low temperature tail of the low field magnetoresistance; (ii) the high field behavior of the magnetoresistance (or the magnetoconductance), and (iii) the AMR behavior.

A model including spin polarized tunneling best explains our experimental results. A tunneling junction can be modeled as a resistor,[31] with the resistance given by $R_j = 1/G_j$, where G_j is the tunneling conductance. The basic building block in our biepitaxial films is therefore $R = R_j + R_e$, where R_e is the resistance of the LSMO ferromagnetic electrodes. For temperatures $T \ll T_c$, $R_j \gg R_e$ holds even though R_e of the biepitaxial film due to lattice strain may be larger than the resistivity of the EF film.

Magnetoresistance measurements on single magnetic tunnel junctions in general show step like features between high and low resistance states of the junction at fields corresponding to the coercive field of the structure.[10,11] For our grain boundary samples, the $\rho(H)$ curves exhibit less sharp features [confer Fig. 6(b)], which is an effect caused by dispersion in the parameters controlling the spin polarized tunneling process.

In the original work of Julliere,[32] an assumption of spin conservation in the tunneling process was made and the magnetoresistance was simply expressed in terms of the spin polarizations $P_{1,2}$ of the two ferromagnetic electrodes; $P = (n\uparrow* - n\downarrow*)/(n\uparrow* + n\downarrow*)$, where $n\uparrow*$ and $n\downarrow*$ are the electronic density of states for majority and minority carriers, respectively. To explain the observed temperature dependence of the magnetoresistance for the films containing grain boundaries, it is necessary to add to the spin conserving tunneling process the possibility of spin-flip tunneling,[15–19] eg., induced by magnetic impurity states inside the barrier[15] or by spin wave excitations at the barrier surface.[18] Another possibility of explaining this temperature dependence is linked to the intrinsic spin polarization[18] in CMR materials. At low temperature, experimental results indicate half-metallic behavior,[33–35] i.e., complete spin polarization ($P_{1,2} = 1$), results which are corroborated by band structure calculations.[36,37] However, the experimental result[33–35] also indicate that the electronic structure varies with temperature. This led Lyu *et al.*[18] to propose a model where the temperature dependent tunneling magnetoresistance is an effect resulting from a temperature dependent spin polarization in combination with collective spin excitations at interfaces. It was also shown that this model could reproduce the main features of the temperature dependent magnetoresistance obtained for a LSMO/STO/LSMO trilayer junction.[10] The similarity between the results shown in Fig. 5 for the temperature dependent magnetoresistance and the results obtained for the trilayer junction suggests that the model of Lyu *et al.*[18] also applies for the GBF and 2DA samples. More specifically, the model correctly predicts a strong decrease of the magnetoresistance at a temperature much lower than T_c.

To be able to account for the high field behavior of the magnetoresistance it is necessary to consider the magnetic properties of the grain boundary itself. Here it should be pointed out that the observed slope of the high field conductance is much larger than that observed for the epitaxial film, and therefore it is not possible to assign this high field behavior to the LSMO electrodes. A linear high field regime for the conductance has previously been reported by Lee *et al.*, who studied the magnetotransport behavior of polycrystalline manganite samples.[9] In the same paper, it was shown that the experimental results were consistent with an interpretation based on second-order tunneling through inter-

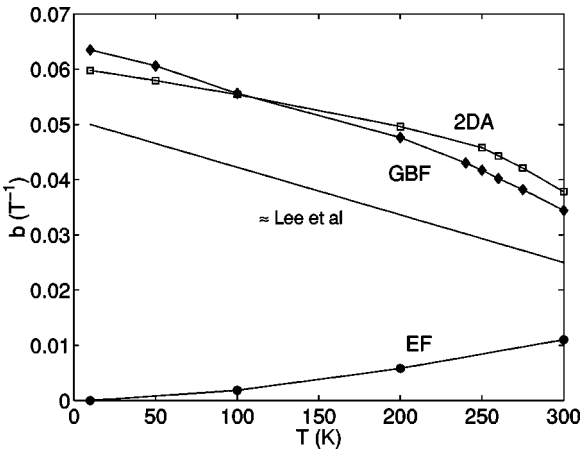

FIG. 9. Temperature dependence of the normalized high field magnetoconductance slope $b(T) = dG/\mu_0 G_0 dH$; Earlier results by Lee *et al.* (Ref. 9) are included for comparison (solid line).

facial spin sites. Using the transfer integral $T_{12} \propto \sqrt{1 + \vec{s_1} \cdot \vec{s_2}}$ for intinerant e_g electrons between localized t_{2g} moments ($\vec{s_1}$ and $\vec{s_2}$ are the normalized spin moments), the conductivity G_j was given as

$$G_j \sim {T_{1j}}^2 {T_{j2}}^2 = \langle (1 + \vec{s_1} \cdot \vec{s_j}) \cdot (1 + \vec{s_j} \cdot \vec{s_2}) \rangle, \qquad (1)$$

where $\vec{s_j}$ is the normalized grain boundary spin moment and $\langle \ldots \rangle$ denotes thermal average. For large enough field, having saturated the magnetization of the two LSMO electrodes, and to lowest order in field, one obtains $G_j \sim \langle \vec{s_j} \rangle \propto \chi_j H$, where χ_j is the susceptibility of the boundary region. Our own results for the biepitaxial films also show that the magnetoconductance, rather than the magnetoresistance, exhibits a linear high field regime. The initial conductivity rise (before the linear regime) at low temperature is close to 30% for 2DA [confer Fig. 5(a)], in agreement with the upper limit of 33 % predicted by the model.

The magnetic properties of the boundaries as given by the temperature dependence of the normalized high field slope of the magnetoconductance $b(T) = dG/\mu_0 G_0 dH \propto \chi_j$ is shown in Fig. 9. The results obtained by Lee *et al.*[9] for a polycrystalline $La_{0.67}Sr_{0.33}MnO_3$ sample are included for comparison. It is noteworthy that the properties of the grain boundaries are so similar in the biepitaxial films and in bulk polycrystalline LSMO samples, indicating that the magnetism close to an interface is determined by intrinsic rather than extrinsic properties. The temperature dependence of the high field χ_j, with a weak increase with decreasing temperature, suggests some kind of disordered magnetic state in the grain boundary region. As to the true nature of this state, it is not possible to give a definite answer only on the basis of the present study. In passing, we note that a different model, not based on spin polarized tunneling, has been proposed by Evetts *et al.*[20] to describe the observed magnetoresistance behavior of artificial grain boundaries in thin film bicrystals. This model depends on activated transport within grain boundary regions, and the magnetoresistive response is determined by the grain boundary magnetization. While this model is capable of explaining some of the features observed for the bi-epitaxial

films, it predicts a linear high-field regime for the resistance rather than for the conductance.

The model, as formulated by Lee *et al.*,[9] does not contain an anisotropic term to relate to the angular profiles of the resistivity shown in Fig. 7. Ziese and Sena[29] developed an atomic model to explain the AMR in CMR materials. In this model the AMR amplitude is expressed in terms of intrinsic local parameters like the spin-orbit coupling, the crystal-field and exchange-field splittings. This implies that both the electrode and the grain boundary near regions exhibit an AMR effect of the same atomic origin. The larger AMR observed for the biepitaxial films can be attributed to stress fields associated with the grain boundaries. The resulting strain may change intrinsic properties such as the crystal-field splitting locally, thereby affecting the AMR amplitude.[29]

Below saturation, the AMR of EF contains 4θ and 6θ terms comparably large in magnitude, something which can be attributed to the symmetry of the magnetic anisotropy. These higher frequency angular terms are rather much smaller in magnitude for GBF, while for 2DA the relative magnitudes of these terms again are large. It is worth noting that this observation cannot be explained by differences in domain configurations and possible domain wall contributions to the magnetoresistance, since the results discussed here correspond to the reversible or near to reversible magnetization regime with the applied field being much larger than the coercive field. The reinforcement of the 4θ and 6θ terms in case of 2DA is instead attributed to the existence of oriented grain boundaries in this film. To account for this, an anisotropic term with the same symmetry as the grain boundary array is included by replacing, as suggested by Evetts *et al.*,[20,38] the applied field with the local field H_j acting on the grain boundary region,

$$\langle \vec{s_j} \rangle = \chi_j (H + f(\phi) M_e), \tag{2}$$

where $f(\phi)$ is a geometric factor and M_e the saturation magnetization of the LSMO electrode. This additional term does not contribute significantly at high fields, so the linear high field behavior of the conductivity is preserved, but adds an orientation dependent term to the conductivity, $f(\phi)$ depending on the orientation of applied field with respect to the grain boundary array. Thus, the reinforcement of the higher frequency angular terms observed for 2DA is a result of creating an artificial square array of grain boundaries in this sample.

V. CONCLUSION

We have compared the magnetic and transport properties of biepitaxial films of $La_{0.7}Sr_{0.3}MnO_3$ with the corresponding properties of a high quality epitaxial film. Both biepitaxial samples exhibit a grain boundary dominated resistivity, and the magnetoresistance results are well described by a two-step spin polarized tunneling mechanism. Additional anisotropic magnetoresistance effects are discussed, and found to have both intrinsic (magnetic anisotropy) and extrinsic (grain boundary distribution) origins. The two-step tunneling model originally proposed by Lee *et al.*[9] is modified to include the anisotropic features. Surprinsingly, for the 2D array, a constant magnetization was observed above the Curie temperature of LSMO, indicating a magnetic ordering of unknown origin.

ACKNOWLEDGMENT

This work was financially supported by The Swedish Natural Science Research Council (NFR).

*Present address: Department of Physics and Astronomy, University of Birmingham, Edgbaston, Birmingham B15 2TT, United Kingdom.

[1] R. von Helmolt, J. Wecker, B. Holzapfel, L. Schultz, and K. Samwerr, Phys. Rev. Lett. **71**, 2331 (1993).

[2] H.Y. Hwang, S-W. Cheong, N.P. Ong, and B. Batlogg, Phys. Rev. Lett. **77**, 2041 (1996).

[3] M.F. Hundley, M. Hawley, R.H. Heffner, Q.X. Jia, J.J. Neumeier, J. Tesmer, J.D. Thompson, and X.D. Wu, Appl. Phys. Lett. **67**, 860 (1995).

[4] J. O'Donnell, M. Onellion, and M.S. Rzchowski, Phys. Rev. B **54**, 6841 (1996).

[5] K. Steenbeck, T. Eick, K. Kirsch, K. O'Donnell, and E. Steinbeiss, Appl. Phys. Lett. **71**, 968 (1997); K. Steenbeck, T. Eick, K. Kirsch, H.-G. Schmidt, and E. Steinbeiss, *ibid.* **73**, 2506 (1998).

[6] R. Shreekala, M. Rajeswari, K. Ghosh, A. Goyal, J.Y. Gu, C. Kwon, Z. Trajanovic, T. Boettcher, R.L. Greene, R. Ramesh, and T. Venkatesan, Appl. Phys. Lett. **71**, 282 (1997).

[7] M. Ziese, G. Heydon, R. Hohne, P. Esquinazi, and J. Dienelt, Appl. Phys. Lett. **74**, 1481 (1997); M. Ziese, Phys. Rev. B **60**, R738 (1999).

[8] Ll. Balcells, J. Fontcuberta, B. Martinez, and X. Obradors, Phys. Rev. B **58**, R14697 (1998).

[9] S. Lee, H.Y. Hwang, B.I. Shraiman, W.D. Ratcliff II, and S-W Cheong, Phys. Rev. Lett. **82**, 4508 (1999).

[10] Yu Lu, X.W. Li, G.Q. Gong, Gang Xiao, A. Gupta, P. Lecoeur, J.Z. Sun, Y.Y. Wang, and V.P. Dravid, Phys. Rev. B **54**, R8357 (1996); X.W. Li, Yu Lu, G.Q. Gong, Gang Xiao, A. Gupta, P. Lecoeur, J.Z. Sun, Y.Y. Wang, and V.P. Dravid, J. Appl. Phys. **81**, 5509 (1997).

[11] J.Z. Sun, W.J. Gallagher, P.R. Duncombe, L. Krusin-Elbaum, R.A. Altman, A. Gupta, Yu Lu, G.Q. Gong, and Gang Xiao, Appl. Phys. Lett. **69**, 3266 (1996).

[12] S.P. Isaac, N.D. Mathur, J.E. Evetts, and M.G. Blamire, Appl. Phys. Lett. **72**, 2038 (1998).

[13] H.S. Wang and Qi Li, Appl. Phys. Lett. **73**, 2360 (1998); H.S. Wang, Qi Li, Kai Liu, and C.L. Chien, *ibid.* **74**, 2212 (1999).

[14] W. Westerburg, F. Martin, S. Friedrich, M. Maier, and G. Jakob, J. Appl. Phys. **86**, 2173 (1999).

[15] R.Y. Gu, D.Y. Xing, and Jinming Dong, J. Appl. Phys. **80**, 7163 (1996).

[16] F. Guinea, Phys. Rev. B **58**, 9212 (1998).

[17] Pin Lyu, D.Y. Xing, and Jinming Dong, Phys. Rev. B **58**, 54 (1998).

[18] Pin Lyu, D.Y. Xing, and Jinming Dong, Phys. Rev. B **60**, 4235 (1999).

[19] J. Inoue and S. Maekawa, J. Magn. Magn. Mater. **198-199**, 167 (1999).

[20] J.E. Evetts, M.G. Blamire, N.D. Mathur, S.P. Isaac, B.-S. Teo, L.F. Cohen, and J.L. Macmanus-Driscoll, Philos. Trans. R. Soc. London, Ser. A **356**, 1593 (1998).

[21] Z. G. Ivanov, R. A. Chakalov, and T. Claeson, in *Multicomponent Oxide Films for Electronics*, edited by M. E. Hawley, D. H. A. Blank, Ch. B. Eom, D. G. Scholm, and S. K. Streiffer, MRS Symposia Proceedings No. 574 (Materials Research Society, Pittsburgh, 1999), pp. 323–328.
[22] K. Char, M.S. Colclough, L.P. Lee, and G. Zaharchuk, Appl. Phys. Lett. **59**, 2177 (1991).
[23] A. L. Vasiliev and Z. G. Ivanov (unpublished).
[24] A.P. Ramirez, J. Phys.: Condens. Matter **9**, 8171 (1997).
[25] H.L. Ju and H. Sohn, Solid State Commun. **102**, 463 (1997).
[26] C. Srinitiwarawong and M. Ziese, Appl. Phys. Lett. **73**, 1140 (1998).
[27] A.J. Millis, P.B. Littlewood, and B.I. Shraiman, Phys. Rev. Lett. **74**, 5144 (1995).
[28] N. Furukawa, J. Phys. Soc. Jpn. **67**, 3214 (1994).
[29] M. Ziese and S.P. Sena, J. Phys.: Condens. Matter **10**, 2727 (1998).
[30] J. N. Eckstein, I. Bozovic, J. O'Donnell, M. Onellion, and M. S. Rzchowski (unpublished).
[31] G. D. Mahan, *Many-Particle Physics* (Plenum, New York, 1981).
[32] M. Julliere, Phys. Lett. **54A**, 225 (1975).
[33] Y. Okimoto, T. Katsufuji, T. Ishikawa, A. Urushibara, T. Arima, and Y. Tokura, Phys. Rev. Lett. **75**, 109 (1995).
[34] J.-H. Park, C.T. Chen, S-W. Cheong, W. Bao, G. Meigs, V. Chakarian, and Y.U. Idzerda, Phys. Rev. Lett. **76**, 4215 (1996).
[35] J.Y.T. Wei, N.C. Yeh, and R.P. Vasques, Phys. Rev. Lett. **79**, 5150 (1997).
[36] W.E. Pickett and D.J. Singh, Phys. Rev. B **53**, 1146 (1996).
[37] S. Satpathy, Z.S. Popovic, and F.R. Vukajlovic, Phys. Rev. Lett. **76**, 960 (1996).
[38] B.-S. Teo, N.D. Mathur, S.P. Isaac, J.E. Evetts, and M.G. Blamire, J. Appl. Phys. **83**, 7157 (1998).